sustainability

MDPI

Article

Experimental Study on the Dynamic Characteristics of Frozen Silty Clay and Its Influencing Factors

Xiyin Zhang *, Binjie Sun, Zhenjiang Xu, Anqi Huang and Jiada Guan

School of Civil Engineering, Lanzhou Jiaotong University, Lanzhou 730070, China
* Correspondence: zhangxiyin@mail.lzjtu.cn

Abstract: Frozen soils are widely distributed in the seismically active regions of northwest China. Under the background of global warming, the study of the dynamic characteristics of frozen soil is very significant for the sustainable development of engineering in cold regions. In this study, the silty clay in the Lanzhou area of northwest China is selected to investigate the dynamic characteristics and its influence factors by dynamic triaxial tests. Various influence factors were considered, including confining pressure, soil temperature, soil water content and loading frequency. The dynamic elastic modulus ratio and reference dynamic strain amplitude increase as confining pressure and soil temperature decrease, and they also increase as soil water content and loading frequency increase. With an increase in confining pressure, soil water content, loading frequency, and a decrease in soil temperature, the damping ratio decreases but the maximum dynamic elastic modulus increases. With an increase in dynamic strain amplitude, the dynamic elastic modulus ratio has a decreasing trend, while the damping ratio has an increasing trend. It was found that the dynamic behaviors are most sensitive to the soil temperature. In addition, the comprehensive influence effect of soil water content, confining pressure, soil temperature, and loading frequency on the maximum dynamic elastic modulus, maximum damping ratio, and reference dynamic strain amplitude of frozen silty clay are analyzed, and the quantitative relationships between them are established. The results can provide evidence for seismic design and safe operation and maintenance of infrastructure in cold regions.

Keywords: stepped cyclic loading; frozen silty clay; dynamic characteristics; soil temperature; water content; loading frequency

Citation: Zhang, X.; Sun, B.; Xu, Z.; Huang, A.; Guan, J. Experimental Study on the Dynamic Characteristics of Frozen Silty Clay and Its Influencing Factors. *Sustainability* **2023**, *15*, 1205. https://doi.org/10.3390/su15021205

Academic Editors: Syed Minhaj Saleem Kazmi and Gianluca Mazzucco

Received: 10 December 2022
Revised: 25 December 2022
Accepted: 6 January 2023
Published: 9 January 2023

1. Introduction

The vast majority of the northern hemisphere is covered by frozen soil [1]. In total, 70% of China's area is located in the frozen soil region, and this reaches total coverage in the northwest of China. There are many transportation projects crossing the cold region in the northwest of China. Typical key projects include the Qinghai–Tibet Railway, Sichuan–Tibet Railway and Qinghai–Tibet Highway, etc. [2–4]. It is known that these cold regions in northwest China are also located in earthquake-prone areas. Some strong earthquakes are appearing in northwestern China [5–7], including the *M*8.0 Kunshan earthquake in 2001, the *M*7.1 Yushu earthquake in 2010, the *M*7.4 Maduo earthquake on 22 May 2021, and the *M*6.9 Menyuan earthquake on 8 January 2022, etc. All of this seismic activity has produced varying degrees of damage to engineering projects in cold regions, including bridges, roads, and tunnels. It can be seen that frozen soil dynamic parameters are the basic factors affecting the frozen soil-structure dynamic interaction, and are also necessary parameters in the seismic design and evaluation of engineering in cold regions [8–10]. Therefore, investigating the dynamic characteristics of frozen soil is very significant for the design and safe operation and maintenance of infrastructure in cold regions with frequent seismic activity and its research is more important in the value of sustainable development in cold regions.

The dynamic behavior of frozen soil is complex and fragile, influenced by the environment, and the dynamic characteristics of frozen soil are receiving increasing attention [11]. The dynamic triaxial test method is widely used for testing the dynamic behavior of frozen soil, of which the step-by-step loading method is mostly adopted [12–14]. In addition, the resonance column method and the ultrasonic detection method are also used in the study of frozen soil dynamic behavior [15,16]. The dynamic elastic modulus reflects the linear deformation capacity of the frozen soil. The damping ratio reflects the energy dissipation capacity of the frozen soil. They are the two parameters of most interest in conducting a seismic evaluation of engineering projects in frozen soil regions. It was found that there exists a threshold for the influence of these soil physical parameters and loading conditions on the dynamic parameters of frozen soil [17,18]. Before the threshold, the dynamic elastic modulus increases with decreasing soil temperature. With decreasing confining pressure, soil water content and loading frequency, the dynamic elastic modulus shows an increasing trend. The tendency of the damping ratio is always opposite to the dynamic elastic modulus. Once these influences reach the threshold, continued changes in these influences have a less pronounced or even opposite trend on the frozen soil dynamic behavior [19,20]. Most of the existing studies have qualitatively discussed the dynamics of frozen soil and its influencing factors. Based on the existing literature [17–20], there is a significant effect of soil temperature on the dynamic parameters of frozen soil. In addition, the effect of soil water content is also considerable.

Some existing studies showed that the dynamic elastic modulus ratio of Qinghai–Tibet clay increased with a decrease in soil temperature, increasing soil water content and loading frequency, while it decreased with an increase in confining pressure [21]. However, it was also found that the dynamic shear modulus ratio of Qinghai–Tibet clay decreased with decreasing soil temperature, increasing soil water content and confining pressure, while it increased with increasing loading frequency [22]. There is apparent disagreement between existing research results. Therefore, large numbers of reasonable experiments are still needed for further analysis of the dynamic characteristics of frozen soil influenced by multi-factors. In addition, some studies have used the equivalent linearization model to fit the prediction equations of the maximum dynamic elastic modulus, the reference dynamic strain amplitude and the maximum damping ratio [19,21,22]. However, these prediction equations are only applicable under specific conditions and have limitations. The selection of the frozen soil dynamic constitutive model is the key to conducting the dynamic response of the soil layer. The Hardin–Drnevich model [23] is often used to describe the dynamic constitutive relationship of frozen soil, but for the dynamic constitutive relationship of some special frozen soils, the Hardin–Drnevich model needs to make corresponding corrections to improve accuracy [24].

Most of the triaxial tests of frozen soil focused on higher confining pressures (more than 0.3 MPa) in previous studies. This study conducted dynamic triaxial tests of frozen silty clay at the confining pressure below 0.3 MPa by using the step-by-step loading method of static stress level and dynamic load amplitude. The effects of soil temperature, soil water content, confining pressure, and loading frequency on the dynamic characteristics of frozen silty clay were considered. The discussed dynamic characteristics include dynamic elastic modulus ratio, reference dynamic strain amplitude, maximum dynamic elastic modulus and damping ratio of frozen silty clay. Finally, based on test results through regression analysis, the formulas for the comprehensive effects of soil water content, confining pressure, soil temperature, and loading frequency on the maximum dynamic elastic modulus, maximum damping ratio, and reference dynamic strain amplitude of frozen silty clay are established.

2. Experiment Design

2.1. Test Equipment

The main technical parameters of the test equipment used in this study are as follows: The confining pressure range is from 0 to 1 MPa; the maximum axial load is 20 kN; the

maximum axial displacement is 100 mm; the loading frequency range is from 0 to 5 Hz; the temperature can be reduced to −40 °C; and the accuracy of the temperature digital display instrument is ±0.01 °C. The test system is shown in Figure 1.

Figure 1. Triaxial test system with temperature-controlled vibration. ① is a pneumatic pump; ② is a temperature control system; ③ is a pressure chamber with temperature monitoring; ④ is a dynamic triaxial testing machine; ⑤ is a data acquisition system; ⑥ is a computer monitor; ⑦ is the transformer of the dynamic triaxial testing machine.

2.2. Test Conditions

Frozen soil is a complex multi-phase and multi-component system, including vapor and air in gaseous phase, mineral particles and ice in solid phase, and unfrozen water in liquid phase. Therefore, when the soil type (mineral particles) is determined, some physical parameters of frozen soil will be greatly influenced by soil temperature and soil water content [25,26]. Thus, three soil water contents (14%, 16%, 18%) and four soil negative temperatures (−0.3 °C, −1 °C, −3 °C, −5 °C) were considered in this study. Previous research showed that the dynamic characteristics of frozen soil were also dependent on the confining pressure, loading frequency, dynamic stress history, etc. [3,13,17–22,24,27]. Therefore, three confining pressures (0.1 MPa, 0.2 MPa, and 0.3 MPa) and three loading frequencies (1 Hz, 2 Hz, 4 Hz) were also taken into account. Furthermore, the dynamic stress history was simulated by step loading and vibration cycles.

2.3. Soil Sample Preparation

In this paper, the soil used was silty clay collected from Lanzhou, a seasonal frozen soil region in northwest China, its basic physical properties are displayed in Table 1 and the particle-size distributions of the tested soils are shown in Figure 2.

Table 1. Physical properties of the soil sample.

Liquid Limit /%	Plastic Limit /%	Plastic Limit Index	Optimum Water Content/%	Dry Density /(g·cm^3)
27.1	14.9	12.2	15.5	1.75

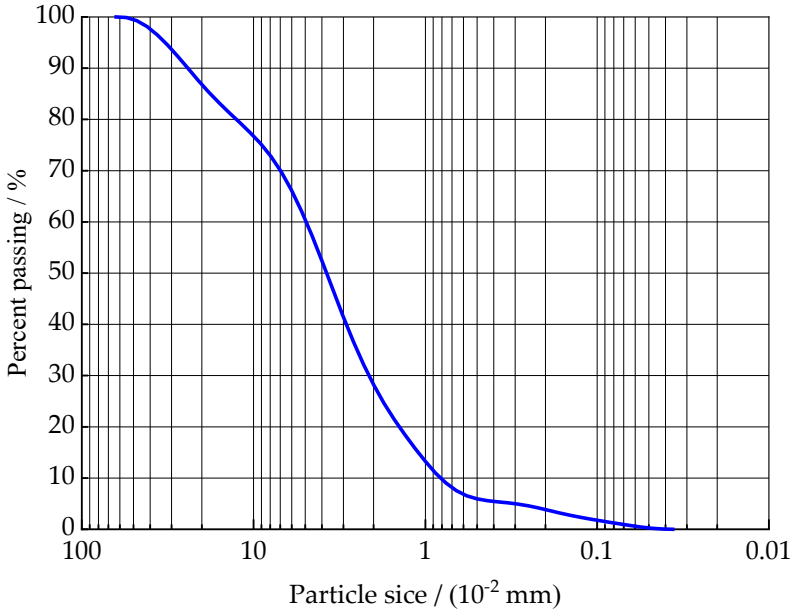

Figure 2. Particle-size distributions of the tested soils.

Soil sample preparation process is as follows, also as shown in Figure 3.

Figure 3. Schematic diagram of soil sample preparation process.

1. The collected soils were crushed and then sieved through a 2 mm square hole sieve, the soil with particle size less than 2 mm was retained and then oven-dried;
2. The dried soils were moistened with the required soil water content for the test and sealed in a plastic bag for twenty-four hours. This will achieve a uniform distribution of water in the soil sample;
3. The prepared soil was pressed into mold in layers. Then, a soil sample is made, which was 100 mm in height and 50 mm in diameter;
4. The prepared soil samples were wrapped in cling film to retain water for testing.

2.4. Loading Procedure

In this paper, the seismic loads are transformed into simple harmonic loads according to the method proposed by Seed [28]. The simple harmonic loads are loaded onto the soil samples using a step-by-step loading approach. The loading schematic diagram is shown in Figure 4. The loading process of each sample has five steps as follows:

- The first step was the consolidation process of soil sample;
- The second step was the freezing process of soil sample, which reduced the temperature to the target value and then held it for 5 h to make the soil temperature reach the target value uniformly;
- The third step was the axial static loading process of soil sample;
- The fourth step was the axial static load maintaining process of soil sample, which was about thirty seconds;
- The fifth step was the axial dynamic loading process of soil sample.

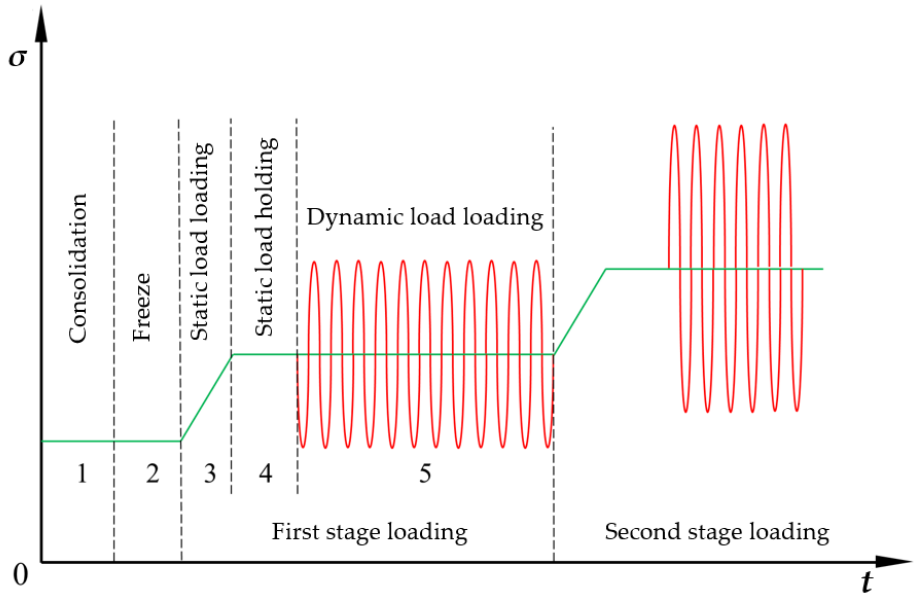

Figure 4. The test loading process.

The soil sample was kept in compression during the whole loading process. For dynamic loading, it vibrated fifteen times in form of a sine wave at each stage, and the equation of sine wave was as follows:

$$\sigma(t) = \sigma_0 + \sigma_m \sin(2\pi f t) \quad (1)$$

where σ_0 is the initial static stress; σ_m is the dynamic stress amplitude; f is the loading frequency; t is the loading time.

Each sample was loaded by increasing the dynamic load amplitude and initial static load step-by-step, and the static stress and dynamic load amplitude increased by the same amount between adjacent loading steps. The specific loading conditions are listed in Table 2.

Table 2. Loading Conditions.

σ_3/MPa	T/°C	σ_0/MPa	σ_{0i}/MPa	σ_{m1}/MPa	σ_m/MPa
0.1		0.166	0.017	0.020	0.010
0.2	−0.3	0.179	0.018	0.022	0.011
0.3		0.191	0.019	0.024	0.012
0.1		0.312	0.037	0.040	0.020
0.2	−1	0.335	0.040	0.050	0.025
0.3		0.358	0.043	0.060	0.030
0.1		0.519	0.073	0.120	0.060
0.2	−3	0.558	0.078	0.130	0.070
0.3		0.597	0.083	0.140	0.080
0.1		0.623	0.073	0.115	0.060
0.2	−5	0.670	0.078	0.125	0.070
0.3		0.717	0.083	0.135	0.050

In table, σ_3 denotes the confining pressure; T denotes the soil temperature; σ_0 denotes the initial static stress; σ_{0i} denotes an increase in the initial static stress of the adjacent level; σ_{m1} denotes the first level dynamic load amplitude; σ_m denotes the increase in dynamic load amplitude of adjacent loading stages.

3. Test Results Analysis

3.1. Calculation of the Dynamic Elastic Modulus Ratio

The schematic diagram of the hysteretic curve of frozen soil is shown in Figure 5. In Figure 5, in order to calculate the corresponding dynamic parameters of the frozen soil, the corresponding auxiliary lines are made on the hysteretic curve based on the intrinsic model suggested by Hardin–Drnevich [23]. The dynamic elastic modulus ratio is calculated as follows [19,21,23]:

$$\sigma_m = \varepsilon_m / (a + b\varepsilon_m) \quad (2)$$

$$E_d = \sigma_m / \varepsilon_m \quad (3)$$

where σ_m is the dynamic stress amplitude, its value is $|JE|/2$; ε_m is the dynamic strain amplitude, its value is $|IC|/2$; and a and b are the testing parameters. Combining Equations (2) and (3), we can obtain Equation (4), the values of a and b can be obtained according to Equation (4), whose physical significance is expressed by Equations (5) and (6).

$$1/E_d = a + b\varepsilon_m \quad (4)$$

$$E_{dmax} = \lim_{\varepsilon_m \to 0} E_d = 1/a \quad (5)$$

$$\sigma_{mult} = \lim_{\varepsilon_m \to \infty} E_d = 1/b \quad (6)$$

where E_{dmax} is the maximum dynamic elastic modulus and σ_{mult} is the ultimate dynamic stress amplitude.

Substituting Equations (5) and (6) into Equation (4), we can obtain Equation (8). ε_{mre} is the reference dynamic strain amplitude.

$$\varepsilon_{mre} = \sigma_{mult} / E_{dmax} = a/b \quad (7)$$

$$E_d = E_{dmax} / (1 + \varepsilon_m / \varepsilon_{mre}) \quad (8)$$

According to Equation (8), the dynamic elastic modulus ratio α_E can be expressed as Equation (9).

$$\alpha_E = E_d / E_{dmax} = 1/(1 + \varepsilon_m / \varepsilon_{mre}) \quad (9)$$

3.2. Calculation of the Damping Ratio

Combined with Figure 5, the damping ratio of frozen soil can be expressed by Equation (10) [23].

$$\lambda = A_L / 4\pi A_T \quad (10)$$

where A_L is the area surrounded by the curve BFHK, which represents the energy lost by the frozen soil material in one loading cycle and A_T is the area of the OAC, which represents the elastic strain energy contained in frozen soil before each loading cycle.

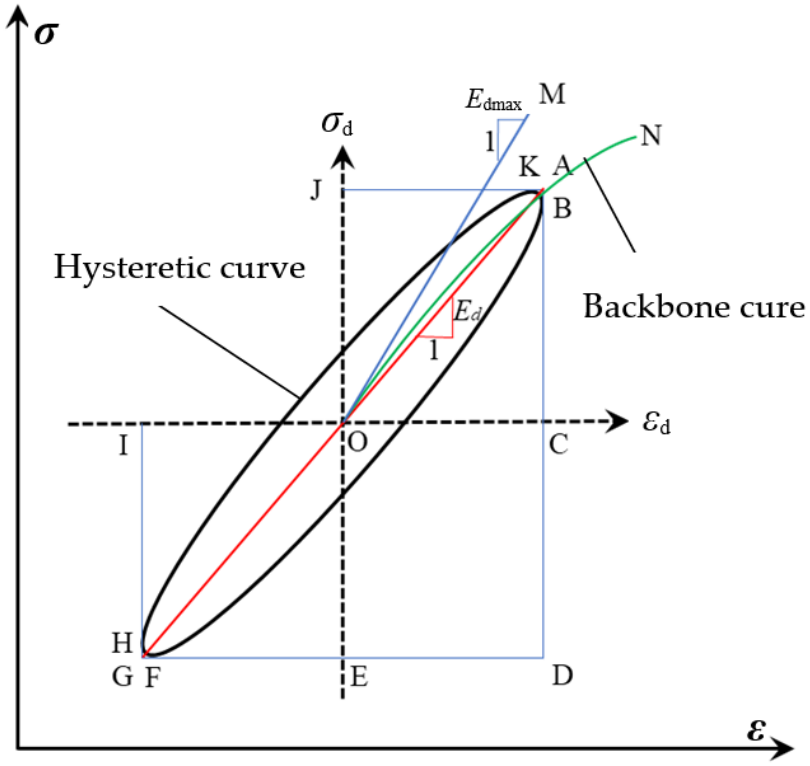

Figure 5. Schematic diagram of ideal hysteretic curve for frozen soil.

It is known that frozen soil is not an ideal viscoelastic material and that there will be residual deformation in every loading cycle, which exhibits an unclosed hysteretic curve, as shown in Figure 6. The start and end points of the hysteresis curve are linked to create a closed polygon, which is used to calculate the energy dissipation [13,18].

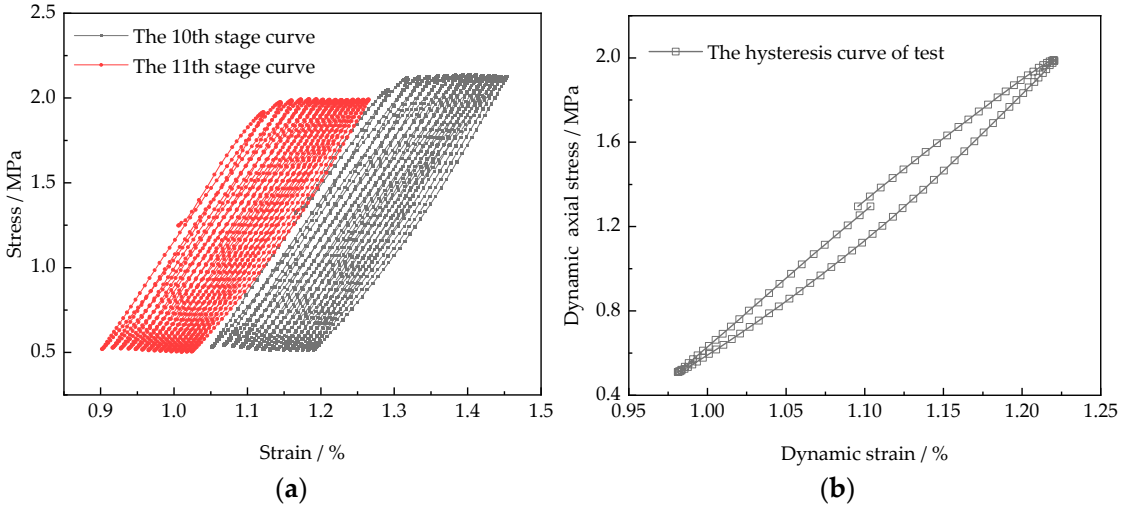

Figure 6. Stress–strain curve of frozen silty clay (w = 16%, f = 4 Hz, T = −3 °C, σ_3 = 0.2 MPa). (**a**) Two stages loading stress–strain curve during actual loading; (**b**) hysteretic curve of frozen soil under one loading cycle.

3.3. Influencing Factors of Frozen Soil Dynamic Parameters

The parameters of the Hardin–Drmevich constitutive model under various conditions of the frozen silty clay are calculated based on the experimental results listed in Table 3. Detailed discussions were carried out in the following text.

Table 3. Summary of Hardin–Drmevich model parameters.

Test Number	w/%	σ_3/MPa	T/°C	f/Hz	a/MPa^{-1}	b/MPa^{-1}	R
1	14	0.1	−3	4	0.001673	0.129900	0.98598
2	14	0.2	−3	4	0.001621	0.147960	0.97962
3	14	0.3	−3	4	0.001589	0.169660	0.98988
4	16	0.1	−3	4	0.001554	0.111020	0.98864
5	16	0.2	−3	4	0.001492	0.123470	0.98789
6	16	0.3	−3	4	0.001444	0.137870	0.99323
7	18	0.1	−3	4	0.001502	0.098240	0.97818
8	18	0.2	−3	4	0.001451	0.107780	0.99114
9	18	0.3	−3	4	0.001398	0.117640	0.97860
10	16	0.1	−1	4	0.002146	0.228830	0.98056
11	16	0.2	−1	4	0.002070	0.240350	0.96288
12	16	0.3	−1	4	0.001955	0.265390	0.97683
13	16	0.1	−5	4	0.001413	0.048020	0.98057
14	16	0.2	−5	4	0.001370	0.053140	0.97937
15	16	0.3	−5	4	0.001351	0.057500	0.96823
16	16	0.1	−3	2	0.001577	0.127120	0.96822
17	16	0.2	−3	2	0.001512	0.132740	0.97889
18	16	0.3	−3	2	0.001468	0.153970	0.97937
19	16	0.1	−3	1	0.001594	0.138660	0.96892
20	16	0.2	−3	1	0.001536	0.156500	0.96785
21	16	0.3	−3	1	0.001488	0.165080	0.96580
22	14	0.3	−3	1	0.001720	0.219620	0.98443
23	14	0.3	−3	2	0.001660	0.199160	0.97865
24	18	0.3	−3	1	0.001530	0.147590	0.96857
25	18	0.3	−3	2	0.001460	0.133200	0.96561
26	16	0.1	−0.3	4	0.003160	0.482560	0.98065
27	16	0.2	−0.3	4	0.002890	0.519520	0.97125
28	16	0.3	−0.3	4	0.002660	0.582858	0.97954

3.4. Confining Pressure

According to Figure 7, the ε_m is within 0.004. The λ tends to increase gradually with an increase in ε_m. The α_E shows a significant decreasing trend with an increase in ε_m. This is because as the loading continues, the soil skeleton is damaged more seriously, which leads to a rapidly decreasing trend in the dynamic elastic modulus. With the destruction of the soil skeleton, the slip between soil particles is easier, which in turn leads to a decrease in the contained energy in the soil and an increase in the dissipated energy in the same vibration period.

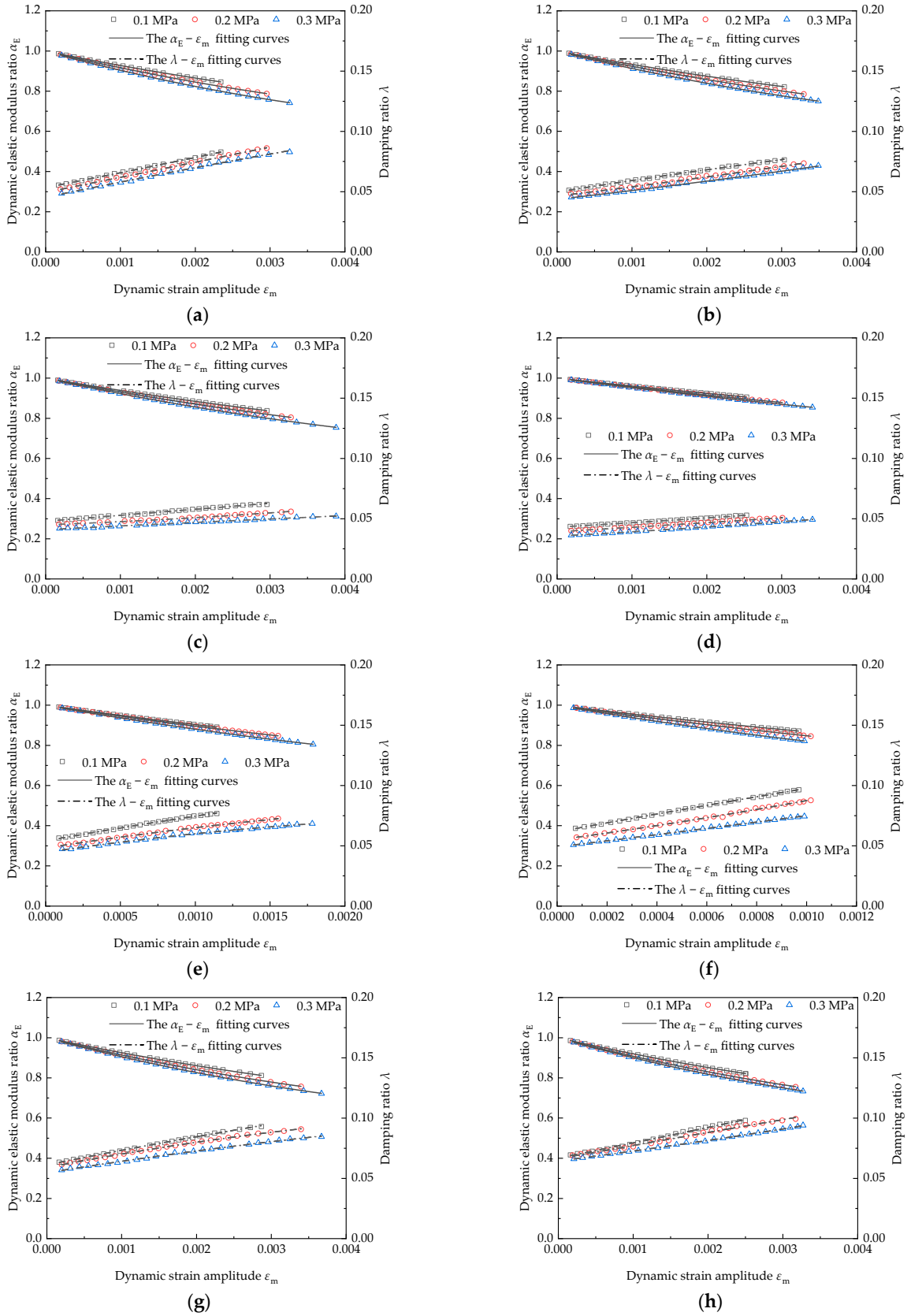

Figure 7. Changing of the α_E and λ with ε_m under different confining pressures. (**a**) w = 14%, f = 4 Hz, T = −3 °C; (**b**) w = 16%, f = 4 Hz, T = −3 °C; (**c**) w = 18%, f = 4 Hz, T = −3 °C; (**d**) w = 16%, f = 4 Hz, T = −5 °C; (**e**) w = 16%, f = 4 Hz, T = −1 °C; (**f**) w = 16%, f = 1 Hz, T = −0.3 °C; (**g**) w = 16%, f = 2 Hz, T = −3 °C; (**h**) w = 16%, f = 1 Hz, T = −3 °C.

The confining pressure has dual effects on the dynamic behaviors of frozen soil, i.e., strengthening and weakening. The reason for the strengthening is that the small cracks between the soil particles will be further compressed and almost closed with an increase in confining pressure. The compacted soil leads to increased friction between the soil particles, which in turn leads to the increased stiffness and strength of the soil. The reason for the weakening is that an increase in confining pressure will lead to the thawing of the ice crystals in the soil. Thawing will lead to soil water migration, a plastic flow phenomenon of the soil particles and reduced cohesion. As a result, the old connection bonds among the soil particles are broken and a new soil skeletal structure is formed. The newly formed soil skeleton stock is still not stable enough. The soil particles more easily slide relative to each other under the action of external forces, thus reducing the strength and stiffness of the soil skeleton.

In this study, the λ shows a gradually decreasing trend with an increase in σ_3, changing from 1.2% to 0.5% and the decreasing trend is more significant with an increasing ε_m. The strengthening effect of the confining pressure gradually enhances with an increase in confining pressure but the weakening effect changes little, which induces an increase in the strength and stiffness. Thus, with an increase in confining pressure, the energy of the frozen soil increases gradually, and the energy dissipation decreases correspondingly during the loading process. According to Equation (9), λ shows a decreasing trend with an increase in confining pressure.

The α_E tends to decrease with an increase in σ_3, which is also related to the strengthening effect. According to Equations (7) and (8), the α_E is related to the ε_{mre}, while the ε_{mre} is related to the parameters of a and b. According to Figure 8, with an increase in σ_3, the void between the soil particles is reduced, which is conducive to improving the friction among the soil particles. Therefore, the E_{dmax} increases with an increasing σ_3, i.e., the parameter a decreases. However, confining pressure also has a weakening effect. In the loading process, the loss of frozen soil strength and stiffness is faster, i.e., the parameter b increases. Therefore, ε_{mre} decreases with an increase in σ_3. According to Equation (8), α_E decreases with a decrease in ε_{mre}. It can be observed that the strengthening effect of confining pressure has a dominant influence on the dynamic behaviors of frozen soil due to the relatively low confining pressure used in this study.

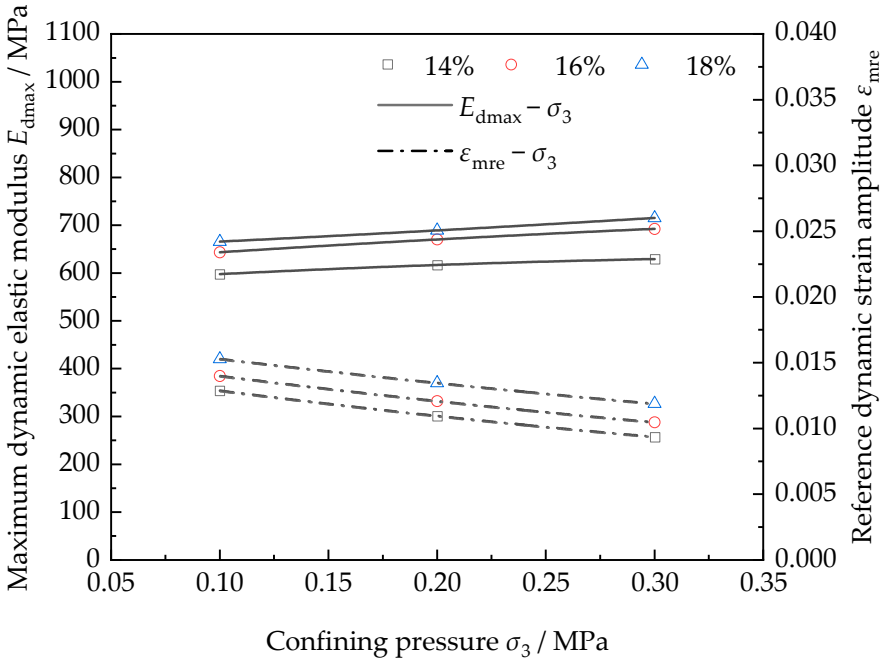

Figure 8. Changing the E_{dmax} and ε_{mre} of different soil water contents with σ_3 (T = −3 °C, f = 4 Hz).

3.5. Soil Temperature

According to Figure 9, λ shows a gradually increasing trend with an increase in ε_m, and its increasing rate slows down with a decrease in soil temperature. λ decreases with a decrease in soil temperature. This is because as the soil temperature decreases, the ratio between the ice and water content in the soil increases, the cementation among the soil particles and ice crystals increases, and the internal skeleton of the frozen soil becomes more stable. Moreover, the energy contained in the frozen soil increases, and the energy dissipation decreases during testing, which leads to a decrease in the damping ratio.

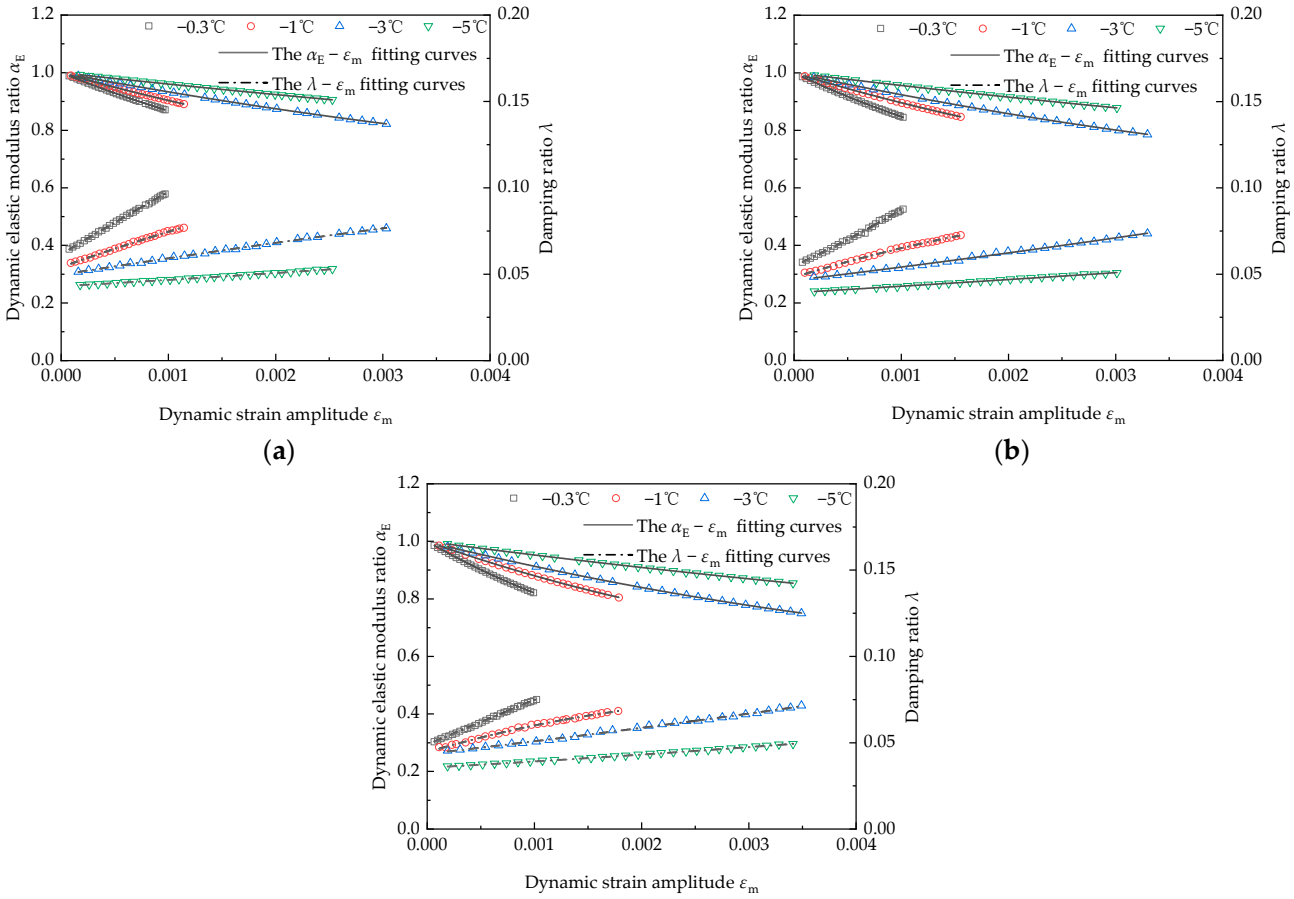

Figure 9. Changing of α_E and λ with ε_m under different soil temperatures. (**a**) w = 16%, f = 4 Hz, σ_3 = 0.1 MPa; (**b**) w = 16%, f = 4 Hz, σ_3 = 0.2 MPa; (**c**) w = 16%, f = 4 Hz, = 0.3 MPa.

According to Figure 10, the decrease in soil temperature enhances the cementation among the soil particles and ice crystals, which results in E_{dmax} and ε_{mre} increasing with a decrease in soil temperature. Therefore, α_E also increases with a decrease in soil temperature. It can also be seen from Figure 10 that the temperature of −3 °C is an inflection point for the variations E_{dmax} and ε_{mre}. When the soil temperature is between −0.3 °C and −3 °C, the E_{dmax} increases rapidly and increases slowly after −3 °C. The increasing rate of ε_{mre} is opposite to the E_{dmax}.

3.6. Soil Water Content

According to Figure 11, the α_E increases and λ decreases with an increase in soil water content. With an increase in soil water content the ice crystals in the soil increase, which can fill part of the pores among the soil particles. The increasing ice crystals can also change the arrangement of the soil particles and increase the friction among the soil particles. Therefore, the damping ratio, stiffness and strength of the soil increase accordingly. From

Figure 12 it also can be seen that E_{dmax} and ε_{mre} increase with an increase in soil water content. The difference in the increasing rate between E_{dmax} and the σ_{mult} leads to an α_E increase with the increase in soil water content.

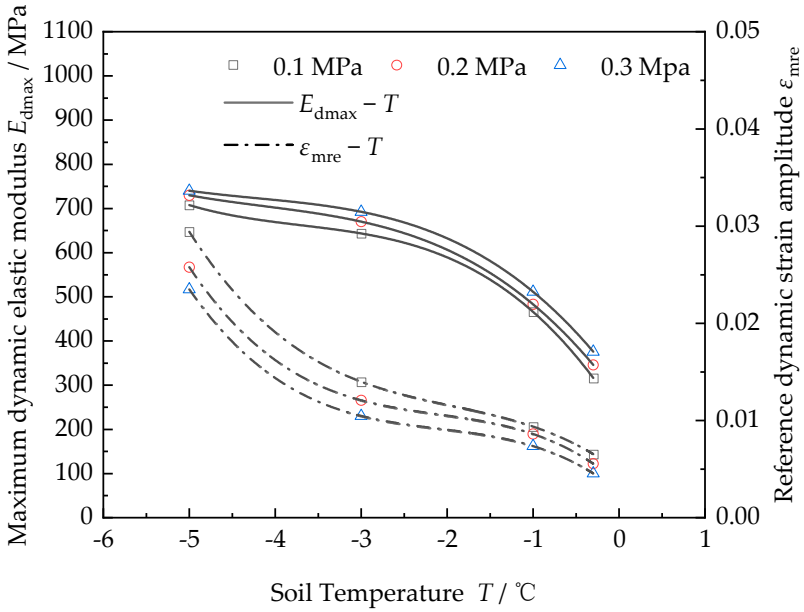

Figure 10. Changing of E_{dmax} and ε_{mre} of different confining pressures with T (w = 16%, f = 4 Hz).

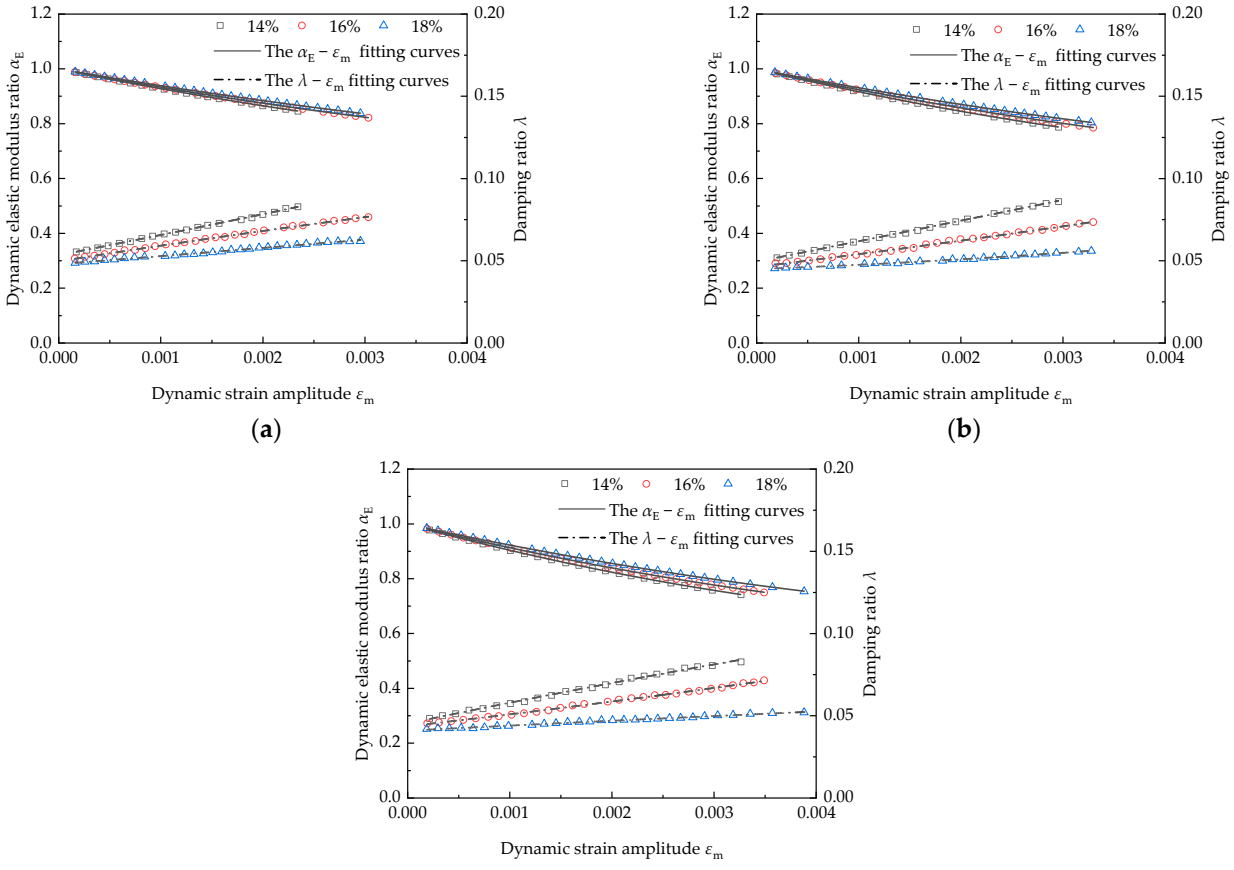

Figure 11. Changing of α_E and λ with ε_m under different soil water contents. (**a**) T = −3 °C, f = 4 Hz, σ_3 = 0.1 MPa; (**b**) T = −3 °C, f = 4 Hz, σ_3 = 0.2 MPa; (**c**) T = −3 °C, f = 4 Hz, = 0.3 MPa.

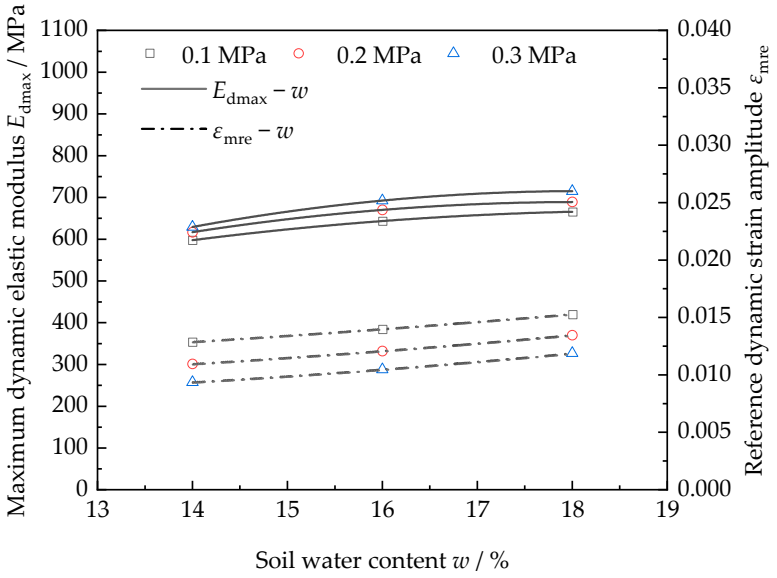

Figure 12. Changing of E_{dmax} and ε_{mre} of different confining pressures with w (T = −3 °C, f = 4 Hz).

3.7. Loading Frequency

It can be seen from Figure 13 that λ decreases significantly with an increase in the loading frequency. The soil deformation shows a hysteretic effect relative to the applied load, and this hysteresis becomes more significant as the frequency increases. If this hysteretic effect is stronger, fewer soil particles under loading will be redistributed, and less damage to the soil skeleton will occur. Therefore, during the loading process, the soil energy dissipation decreases and λ decreases with an increase in loading frequency. The α_E also has a slight increase with increasing loading frequency. Because a larger loading frequency will produce a larger hysteresis between the applied load and the corresponding soil deformation, it will further affect the reference dynamic strain amplitude.

As shown in Figure 14, with an increase in loading frequency, the ε_m of frozen soil increases slightly, but the maximum dynamic elastic modulus changes indistinctively. The reason for this is that loading frequency has little effect on parameter a in Equation (4). However, during the loading process, the strength and stiffness of the frozen soil are less likely to be lost as the loading frequency increases, as parameter b decreases accordingly. Therefore, it can be seen from Equations (7)–(9) that the ε_{mre} of frozen soil increases with an increase in the loading frequency and α_E also increases accordingly.

3.8. The Comprehensive Influence Effects

Based on the above discussion, the influencing factors affecting the dynamic behavior of frozen silty clay were standardized and dimensionless. Then, through regression analysis, the relationship for the comprehensive effect of T, w, σ_3, and f on the maximum dynamic elastic modulus, maximum damping ratio, and reference dynamic strain amplitude of frozen silty clay was established. The equations are as follows:

$$E_{dmax} = 670.2413\zeta_w\zeta_{\sigma_3}\zeta_T\zeta_f \quad (11)$$

$$\lambda_{min} = 0.04586\beta_w\beta_{\sigma_3}\beta_T\beta_f \quad (12)$$

$$\varepsilon_{mre} = 0.012084\alpha_w\alpha_{\sigma_3}\alpha_T\alpha_f \quad (13)$$

where E_{dmax} is the value of maximum dynamic elastic modulus in MPa; λ_{min} is the minimum damping ratio; ζ_w, ζ_{σ_3}, ζ_T, ζ_f, respectively, denote the correction coefficients of water content, confining pressure, soil temperature, and loading frequency of the maximum dynamic elastic modulus; and its specific calculation is shown in Equation (14). Similarly, β_w, β_{σ_3}, β_T, β_f, respectively, denote the correlation correction coefficients of the maximum

damping ratio, which are calculated in Equation (15). α_w, α_{σ_3}, α_T, α_f are the correlation correction coefficients of the reference dynamic strain amplitude, which are calculated in Equation (16).

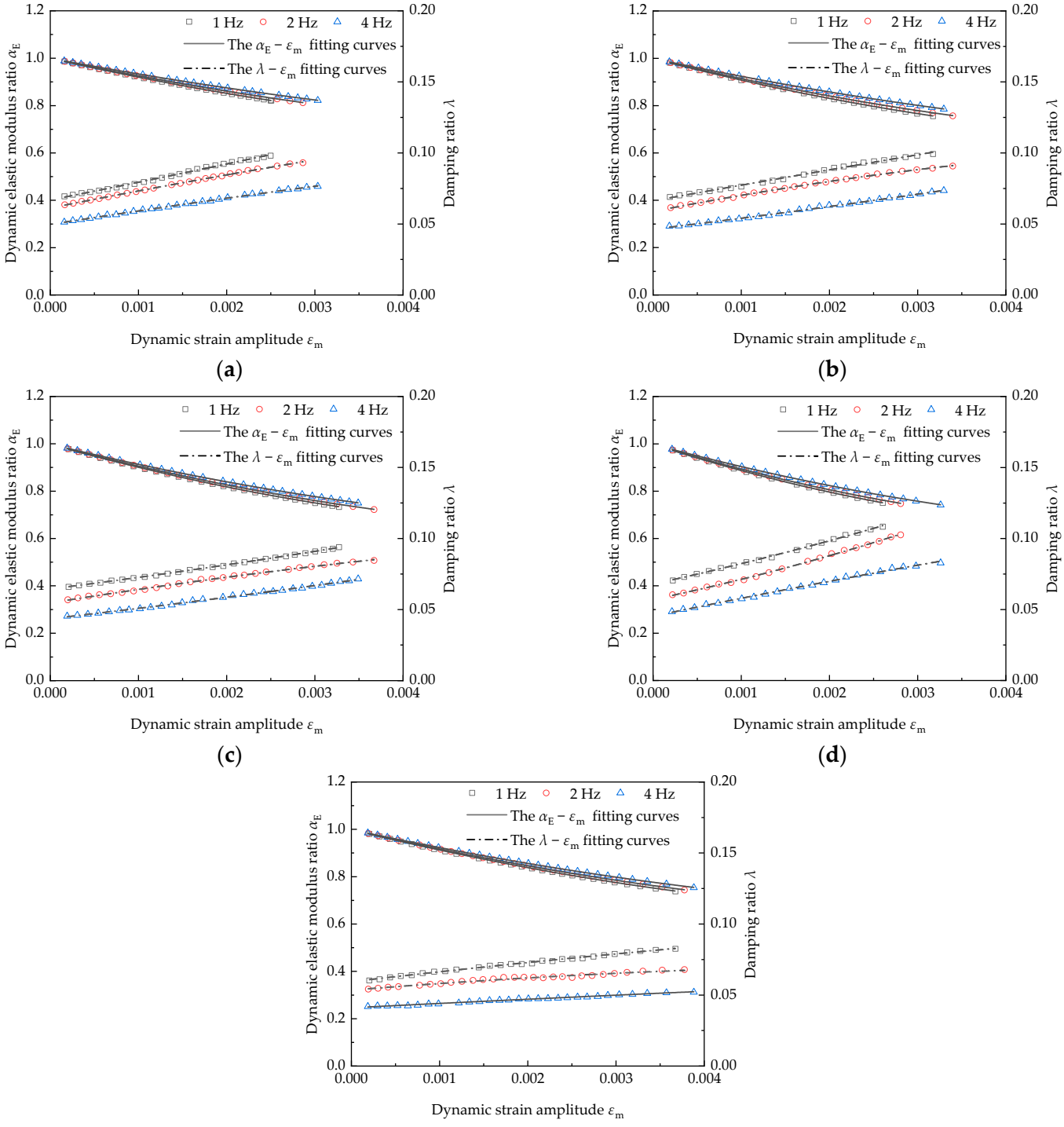

Figure 13. Changing of α_E and λ with ε_m under different loading frequencies. (**a**) w = 16%, T = −3 °C, σ_3 = 0.1 MPa; (**b**) w = 16%, T = −3 °C, σ_3 = 0.2 MPa; (**c**) w = 16%, T = −3 °C, σ_3 = 0.3 MPa; (**d**) w = 14%, T = −3 °C, σ_3 = 0.3 Mpa; (**e**) w = 18%, T = −3 °C, σ_3 = 0.3 MPa.

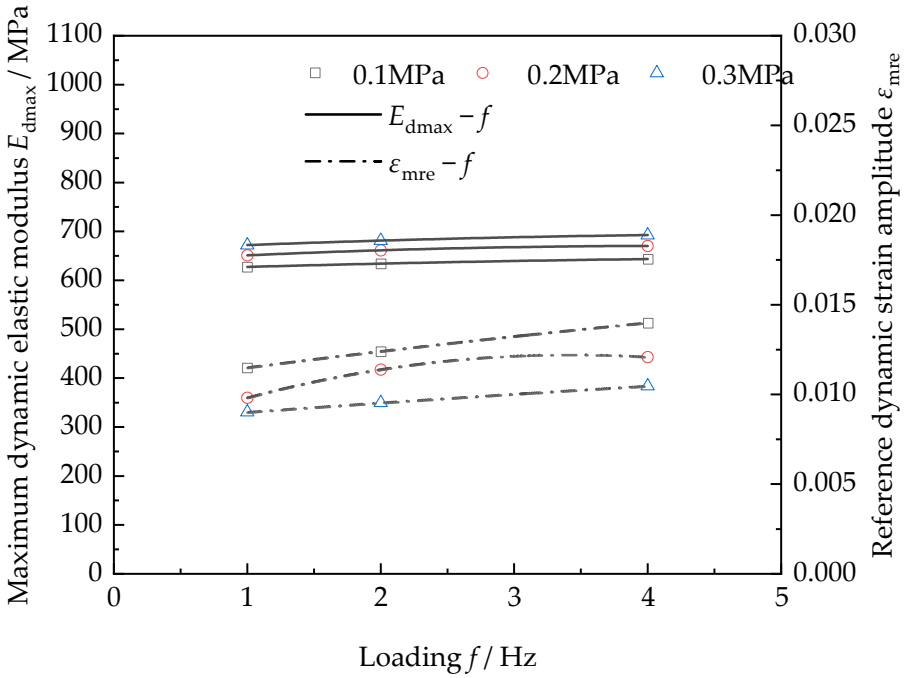

Figure 14. Changing of E_{dmax} and ε_{mre} of different confining pressures with f (T = −3 °C, w = 16%).

$$\begin{cases} \zeta_w = -64.15533w^2 + 23.22563w - 1.07372 \\ \zeta_{\sigma_3} = -0.29902\overline{\sigma}_3^2 + 0.50699\overline{\sigma}_3 + 0.91056 \\ \zeta_T = -0.028148\overline{T}^2 - 0.26663\overline{T} + 0.45562 \\ \zeta_f = -0.0040664\overline{f}^2 + 0.03689\overline{f} + 0.9175 \end{cases} \quad (14)$$

$$\begin{cases} \beta_w = 77.68227w^2 - 27.26238w + 3.37331 \\ \beta_{\sigma_3} = -0.026299\overline{\sigma}_3^2 - 0.77518\overline{\sigma}_3 + 1.15609 \\ \beta_T = -0.0024732\overline{T}^2 + 0.049859\overline{T} + 1.16934 \\ \beta_f = -0.0037607\overline{f}^2 - 0.12942\overline{f} + 1.57783 \end{cases} \quad (15)$$

$$\begin{cases} \alpha_w = 25.90818w^2 - 3.104082w + 0.8334 \\ \alpha_{\sigma_3} = 0.5341\overline{\sigma}_3^2 - 1.58198\overline{\sigma}_3 + 1.295034 \\ \alpha_T = -0.039597\overline{T}^3 - 0.250596\overline{T}^2 - 0.6312633\overline{T} + 0.2924556 \\ \alpha_f = -0.0210076\overline{f}^2 + 0.1620266\overline{f} + 0.6880157 \end{cases} \quad (16)$$

where $\overline{\sigma}_3$ denotes the dimensionless confining pressure and its value is the confining pressure in MPa divided by 1 MPa; $\overline{T}$ denotes the dimensionless soil temperature and its value is the soil temperature in °C divided by 1 °C; and $\overline{f}$ denotes the dimensionless loading frequency and its value is the loading frequency in Hz divided by 1 Hz.

The comprehensive influence equations of frozen silty clay dynamic parameters proposed in this paper are formally referenced to the equation proposed for the frozen Qinghai–Tibet clay dynamic parameters [19]. The experimental and predicted values of the dynamic parameters of the frozen silty clay are summarized in Table 4. From Table 4 it can be seen that the accuracy of the fit is basically controlled below 5% or even smaller, and only the predicted values of the dynamic parameters of individual specimens exceed 5%. However, it is not large as the maximum is 8.19%. All in all, these formulas have high fitting accuracy.

Table 4. Summary of the experimental values compared with the values calculated by the fitted formula.

w /%	σ_3 /MPa	T /°C	f /Hz	$E_{dmax,\ R}$	$E_{dmax,\ F}$	R/%	$\lambda_{min,\ R}$	$\lambda_{min,\ F}$	R/%	$\varepsilon_{mre,\ R}$	$\varepsilon_{mre,\ F}$	R/%
14	0.1	−3	4	597.7286	592.4479	0.88	0.0533	0.0534	0.19	0.0129	0.0125	3.10
14	0.2	−3	4	616.9031	618.2464	0.22	0.0494	0.0495	0.20	0.0110	0.0110	0.00
14	0.3	−3	4	629.3266	640.3475	1.75	0.0460	0.0456	0.87	0.0094	0.0095	1.06
16	0.1	−3	4	643.5006	643.6714	0.03	0.0503	0.0495	1.59	0.0140	0.0138	1.43
16	0.2	−3	4	670.2413	671.7005	0.22	0.0459	0.0459	0.00	0.0121	0.0121	0.00
16	0.3	−3	4	692.5208	695.7125	0.46	0.0431	0.0423	1.86	0.0105	0.0105	0.00
18	0.1	−3	4	665.7790	661.8592	0.59	0.0480	0.0487	1.46	0.0153	0.0154	0.65
18	0.2	−3	4	689.1799	690.6802	0.22	0.0444	0.0451	1.58	0.0135	0.0135	0.00
18	0.3	−3	4	715.3076	715.3707	0.01	0.0412	0.0416	0.97	0.0119	0.0117	1.68
16	0.1	−1	4	465.9832	445.8027	4.33	0.0546	0.0555	1.65	0.0094	0.0098	4.26
16	0.2	−1	4	483.0918	465.2154	3.70	0.0494	0.0514	4.05	0.0086	0.0086	0.00
16	0.3	−1	4	511.5090	481.8460	5.80	0.0463	0.0474	2.38	0.0074	0.0075	1.35
16	0.1	−5	4	707.7141	696.9107	1.53	0.0429	0.0426	0.70	0.0294	0.0294	0.00
16	0.2	−5	4	729.9270	727.2581	0.37	0.0392	0.0395	0.77	0.0258	0.0258	0.00
16	0.3	−5	4	740.1925	753.2562	1.76	0.0353	0.0364	3.12	0.0235	0.0224	4.68
16	0.1	−3	2	634.1154	627.5904	1.03	0.0619	0.0646	4.36	0.0124	0.0128	3.23
16	0.2	−3	2	661.3757	654.9192	0.98	0.0606	0.0599	1.16	0.0114	0.0112	1.75
16	0.3	−3	2	681.1989	678.3314	0.42	0.0558	0.0552	1.08	0.0095	0.0097	2.11
16	0.1	−3	1	627.3526	611.6976	2.50	0.0667	0.0715	7.20	0.0115	0.0114	0.87
16	0.2	−3	1	651.0417	638.3344	1.95	0.0667	0.0664	0.45	0.0098	0.0100	2.04
16	0.3	−3	1	672.0430	661.1536	1.62	0.0638	0.0611	4.23	0.0090	0.0087	3.33
14	0.3	−3	1	581.3953	608.5388	4.67	0.0667	0.0659	1.20	0.0078	0.0079	1.28
14	0.3	−3	2	602.4096	624.3496	3.64	0.0551	0.0595	7.99	0.0083	0.0088	6.02
18	0.3	−3	1	653.5948	679.8353	4.01	0.0600	0.0601	0.17	0.0104	0.0097	6.73
18	0.3	−3	2	684.9315	697.4984	1.83	0.0545	0.0542	0.55	0.0110	0.0109	0.91
16	0.1	−0.3	4	316.4557	342.3799	8.19	0.0619	0.0573	7.43	0.0065	0.0064	1.54
16	0.2	−0.3	4	346.0208	357.2890	3.26	0.0538	0.0531	1.30	0.0056	0.0056	0.00
16	0.3	−0.3	4	375.9398	370.0614	1.56	0.0490	0.0490	0.00	0.0046	0.0048	4.35

In table, $E_{dmax,\ R}$ denotes the maximum dynamic elastic modulus by the testing; $E_{dmax,\ F}$ denotes the maximum dynamic elastic modulus by the fitting formula calculated; $\lambda_{min,\ R}$ denotes the minimum damping ratio by the testing; $\lambda_{min,\ F}$ denotes the minimum damping ratio by the fitting formula calculated; $\varepsilon_{mre,\ R}$ denotes the reference dynamic strain amplitude by the testing; $\varepsilon_{mre,\ F}$ denotes reference dynamic strain amplitude by the fitting formula calculated; R denotes the error rate between the experimental value and the value calculated by the fitted formula.

The research results of this paper expand the content of the dynamic parameters of frozen silty clay with an enclosing pressure of 0.3 MPa or less.

4. Discussion

This paper conducted dynamic triaxial tests to investigate the dynamic characteristics of frozen silty clay and its influencing factors. The factors considered in this study included three confining pressures (0.1 MPa, 0.2 MPa, 0.3 MPa), four soil temperatures (−0.3 °C, −1 °C, −3 °C, −5 °C), three soil water contents (14%, 16%, 18%) and three vibration frequencies (1 Hz, 2 Hz, 4 Hz). Some important conclusions are drawn as follows:

1. With an increase in dynamic strain amplitude, the damping ratio of frozen silty clay shows an increasing trend, and the dynamic elastic modulus ratio tends to decrease. This variation trend is also affected by soil temperature, soil water content, loading frequency and other factors;
2. The damping ratio and reference dynamic strain amplitude of frozen silty clay decreases with an increase in confining pressure, while the dynamic elastic modulus ratio and maximum dynamic elastic modulus tend to increase;
3. Soil temperature is one of the most important factors. With a decrease in soil temperature, the dynamic elastic modulus ratio, maximum dynamic elastic modulus and reference dynamic strain amplitude of frozen silty clay show an increasing trend, while the damping ratio has a decreasing trend. Moreover, the dynamic elastic modu-

lus ratio and damping ratio tend to change gently with the dynamic strain amplitude when the soil temperature increases;

4. With an increase in soil water content, the dynamic elastic modulus ratio, maximum dynamic elastic modulus and reference dynamic strain amplitude of frozen silty clay tend to increase, while the damping ratio tends to decrease. Moreover, the dynamic elastic modulus ratio and damping ratio tend to change gently with a change in soil water content. If the soil water content is below 16%, the effect of confining pressure on the dynamic characteristics of frozen soil will become more obvious;
5. With an increase in loading frequency, the dynamic elastic modulus ratio and reference dynamic strain amplitude tend to increase slightly, while the damping ratio decreases obviously. Moreover, the dynamic elastic modulus ratio and damping ratio change gently with the dynamic strain amplitude when the loading frequency increases;
6. Based on the testing results, the comprehensive influence effects of soil water content, confining pressure, soil temperature, and loading frequency on the maximum dynamic elastic modulus, maximum damping ratio, and reference dynamic strain amplitude of frozen silty clay were analyzed, and the quantitative relationship among the dynamic parameters and their influencing factors were established.

Author Contributions: X.Z.: Methodology, Funding acquisition, Investigation, Formal analysis, Writing—original draft, Writing—review and editing; B.S.: Data curation, Formal analysis, Investigation, Writing—original draft; A.H.: Data curation, Resources; Z.X.: Data curation, Investigation, Resources; J.G.: Data curation, Resources. All authors have read and agreed to the published version of the manuscript.

Funding: This research is supported by the National Natural Science Foundation of China (Grant Nos. U21A2012, 52068045), the Science and Technology Program of Gansu Province for Distinguished Young Scholars (No. 20JR5RA430), the Special Funds for Guiding Local Scientific and Technological Development by The Central Government (No. 22ZY1QA005), and the Science and Technology Research and Development Plan of China State Railway Group Co., Ltd. (P2021G047).

Institutional Review Board Statement: Not applicable.

Informed Consent Statement: Not applicable.

Data Availability Statement: All data, models, and code generated or used during the study appear in the submitted article.

Conflicts of Interest: On behalf of all authors, the corresponding author states that there are no conflicts of interest.

References

1. Zhang, T.; Barry, R.G.; Knowles, K.; Heginbottom, J.A.; Brown, J. Statistics and characteristics of permafrost and Ground-Ice distribution in the Northern Hemisphere. *Polar Geogr.* **2008**, *31*, 47–68. [CrossRef]
2. Wu, Q.; Niu, F.; Ma, W.; Liu, Y. The effect of permafrost changes on embankment stability along the Qinghai–Xizang Railway. *Environ. Earth Sci.* **2014**, *71*, 3321–3328. [CrossRef]
3. Lu, C.; Cai, C. Challenges and Countermeasures for Construction Safety during the Sichuan–Tibet Railway Project. *Engineering* **2019**, *5*, 833–838. [CrossRef]
4. Wu, Q.; Liu, Y.; Zhang, J.; Tong, C. A review of recent frozen soil engineering in permafrost regions along Qinghai-Tibet Highway, China. *Permafr. Periglac. Process.* **2002**, *13*, 199–205.
5. Cui, D.; Wang, Q.; Wang, W. Effect of Kunlun Ms 8.1 earthquake on crustal deformation in northeastern edge region of Qinghal-Tibet plateau. *Geod. Geodyn.* **2010**, *1*, 34–41. [CrossRef]
6. Ni, S.; Wang, W.; Li, L. The April 14th, 2010 Yushu earthquake, a devastating earthquake with foreshocks. *Sci. China Earth Sci.* **2010**, *53*, 791–793. [CrossRef]
7. Deng, Q.; Cheng, S.; Ma, J.; Du, P. Seismic Activities and Earthquake Potential in the Tibetan Plateau. *Chin. J. Geophys.* **2014**, *57*, 678–697. [CrossRef]
8. Fu, R.-H.; Briseghella, B.; Xue, J.-Q.; Aloisio, A.; Lin, Y.-B.; Nuti, C. Experimental and finite element analyses of laterally loaded RC piles with pre-Hole filled by various filling materials in IABs. *Eng. Struct.* **2022**, *272*, 114991. [CrossRef]
9. Guan, J.; Zhang, X.; Chen, X.; Ding, M.; Wang, W.; Yu, S. Influence of seasonal freezing-thawing soils on seismic performance of high-rise cap pile foundation in permafrost regions. *Cold Reg. Sci. Technol.* **2022**, *199*, 103581. [CrossRef]

10. Zhang, X.; Yang, Z.; Chen, X.; Guan, J.; Pei, W.; Luo, T. Experimental study of frozen soil effect on seismic behavior of bridge pile foundations in cold regions. *Structures* **2021**, *32*, 1752–1762. [CrossRef]
11. Ma, D.; Xiang, H.; Ma, Q.; Kaunda, E.E.; Huang, K.; Su, Q.; Yao, Z. Dynamic Damage Constitutive Model of Frozen Silty Soil with Prefabricated Crack under Uniaxial Load. *J. Eng. Mech.* **2021**, *147*, 04021033. [CrossRef]
12. Shastri, A.; Sánchez, M.; Gai, X.; Lee, M.Y.; Dewers, T. Mechanical behavior of frozen soils: Experimental investigation and numerical modeling. *Comput. Geotech.* **2021**, *138*, 104361. [CrossRef]
13. Ling, X.; Li, Q.; Wang, L.; Zhang, F.; An, L.; Xu, P. Stiffness and damping radio evolution of frozen clays under long-term low-Level repeated cyclic loading: Experimental evidence and evolution model. *Cold Reg. Sci. Technol.* **2013**, *86*, 45–54. [CrossRef]
14. Czajkowski, R.L.; Vinson, T.S. Dynamic Properties of Frozen Silt Under Cyclic Loading. *J. Geotechn. Eng. Div.* **1980**, *106*, 963–980. [CrossRef]
15. Wang, D.; Zhu, Y.; Ma, W.; Niu, Y. Application of ultrasonic technology for Physical–Mechanical properties of frozen soils. *Cold Reg. Sci. Technol.* **2006**, *44*, 12–19. [CrossRef]
16. Al-Hunaidi, M.; Chen, P.; Rainer, J.; Tremblay, M. Shear moduli and damping in frozen and unfrozen clay by resonant column tests. *Can. Geotech. J.* **2011**, *33*, 510–514. [CrossRef]
17. Luo, F.; Zhao, S.; Ma, W.; Jiao, D.; Kong, X. Experimental study on dynamic elastic modulus of frozen soils under stepped axial cyclic loading. *Chin. J. Geotech. Eng.* **2013**, *35*, 849–855.
18. Zhao, S.; Zhu, Y.; He, P.; Wang, D. Testing study on dynamic mechanics parameters of frozen soil. *Chin. J. Rock Mech. Eng.* **2003**, *22*, 2677–2681.
19. Zhu, Z.; Ling, X.; Wang, Z.; Lu, Q.; Chen, S.; Zou, Z.; Guo, Z. Experimental investigation of the dynamic behavior of frozen clay from the Beiluhe subgrade along the QTR. *Cold Reg. Sci. Technol.* **2011**, *69*, 91–97. [CrossRef]
20. Zhao, F.; Chang, L.; Zhang, W. Experimental investigation of dynamic shear modulus and damping ratio of Qinghai-Tibet frozen silt under multi-stage cyclic loading. *Cold Reg. Sci. Technol.* **2020**, *170*, 102938. [CrossRef]
21. Ling, X.; Zhu, Z.; Zhang, F.; Chen, S.; Wang, L.; Gao, X.; Lu, Q. Dynamic elastic modulus for frozen soil from the embankment on Beiluhe Basin along the Qinghai–Tibet Railway. *Cold Reg. Sci. Technol.* **2009**, *57*, 7–12. [CrossRef]
22. Wu, Z.; Zhang, D.; Zhao, T.; Ma, J.; Zhao, D. An experimental research on damping ratio and dynamic shear modulus ratio of frozen silty clay of the Qinghai-Tibet engineering corridor. *Transp. Geotech.* **2019**, *21*, 100269. [CrossRef]
23. Hardin Bobby, O.; Drnevich Vincent, P. Shear Modulus and Damping in Soils: Design Equations and Curves. *J. Soil Mech. Found. Div.* **1972**, *98*, 667–692. [CrossRef]
24. Yu, X.; Liu, H.; Sun, R.; Yuan, X. Improved Hardin-Drnevich model for the dynamic modulus and damping ratio of frozen soil. *Cold Reg. Sci. Technol.* **2018**, *153*, 64–77. [CrossRef]
25. Cui, L.; Li, G.; He, Y.; Liao, Q.; Luo, F. Status Analysis of the Frozen Soil's Dynamics Parameter Study. *Adv. Mater. Res.* **2014**, *941–944*, 2626–2630. [CrossRef]
26. Zhang, D.; Li, Q.; Liu, E.; Liu, X.; Zhang, G.; Song, B. Dynamic properties of frozen silty soils with different coarse-grained contents subjected to cyclic triaxial loading. *Cold Reg. Sci. Technol.* **2019**, *157*, 64–85. [CrossRef]
27. Ling, X.; Zhang, F.; Li, Q.; An, L.; Wang, L. Dynamic shear modulus and damping ratio of frozen compacted sand subjected to freeze–thaw cycle under multi-stage cyclic loading. *Soil Dyn. Earthq. Eng.* **2015**, *76*, 111–121. [CrossRef]
28. Seed, H.B.; Idriss Izzat, M. Simplified Procedure for Evaluating Soil Liquefaction Potential. *J. Soil Mech. Found. Div.* **1971**, *97*, 1249–1273. [CrossRef]